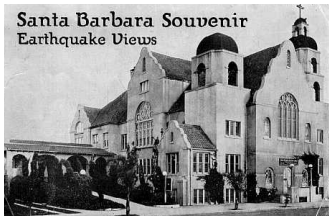

4th IASPEI / IAEE International Symposium:

Effects of Surface Geology on Seismic Motion

August 23–26, 2011 · University of California Santa Barbara

STRESS DROP VARIABILITY AND SITE EFFECTS AT THE BORREGO VALLEY DOWNHOLE ARRAY

Jorge Crempien
University of California
Santa Barbara, CA 93106
USA

Ralph Archuleta
University of California
Santa Barbara, CA 93106
USA

ABSTRACT

Using short-period P waves, Shearer, Prieto and Hauksson (2006) estimated stress drops for ~65,000 earthquakes with $1.6<M_w<3.1$ in southern California. The median stress drop between 8 and 18 km depth is approximately ~2.2 MPa. In their map of smoothed stress drops the stress drop decreases going from west (near the Elsinore Fault) —with values near 1.6 to 2.5 MPa— to east near the southern extension of the San Jacinto Fault and the Imperial Fault —with values near ~0.6 MPa.

The northern end of the El Mayor earthquake was particularly active in producing earthquakes with $M_w>4$. The epicenters are in a region where one would expect stress drops to be as low as ~0.6 MPa. These aftershocks, with $4.0<M_w<5.5$ are well recorded at the Borrego Valley Downhole Array (BVDA) (Steidl, 2006). BVDA has accelerometers at different depths as well as a surface array. We use the accelerograms recorded at depth to compute the spectra of the S waves from which we determine the corner frequency and stress drops using Brune's (1970, 1971) relations. Shearer et al. used Madariaga's (1976) relationship between corner frequency and source radius. Madariaga's relation amplifies the stress drop by 5.5 compared to Brune's.

We have analyzed 27 events of the 2010 El Mayor aftershock sequence with magnitudes between $4.0<M_w<5.5$. Although the epicentral distance ranges between 80 km and 190 km, the backazimuth is nearly constant. We used Q values reported by Hauksson and Shearer (JGR, 2006) to correct the spectrum for each aftershock with a value of Qs = 450. We used accelerograms at the depth of 139 m to avoid site effects. We used a nonlinear least square method to find the best fitting ω^2-model (Aki, 1967; Brune 1970) to the source spectra and determine the corner frequencies for all events. From the original 35 events, we selected 22 recordings with a good fit of the ω^2-model to the observed displacement spectra. The preliminary result for average stress drop is approximately 3.44 MPa, a value that is almost ~32 times as the one reported by Shearer et al. (2006) for this region is southern California if one considers the difference between Madariaga's (1976) relationship with respect to Brune's (1970, 1971) results.

INTRODUCTION

Stress drop is the average difference between initial and final stress along a fault after an earthquake. It is a critical parameter directly related to the level of high frequency ground shaking for a given seismic moment (Frankel, 2009). Based on the assumption that all earthquakes have the same stress drop, Aki (1967) proposed that earthquakes are self-similar. In this seminal work, he argued that earthquakes depend on a single parameter, which scales the dimensional parameters of the faulting and the spectral parameters. The scaling parameter used in Aki's (1967) study was the surface wave magnitude M_s. He concluded that constant stress drop for all earthquakes might be a too strong of an assumption for different tectonic regimes; he suggested a different stress drop should be assumed for each specific tectonic environment.

Stress drop is a key parameter for prediction of broadband time-histories. There are several approaches to simulate strong ground shaking by stitching low-frequency synthetics with high-frequency Green's functions, either synthetic (Hutchings, 1994; Pitarka et al., 2000; Kamae et al., 2005; Frankel, 2009; Graves & Pitarka, 2010) or empirical (Hartzell, 1978; Irikura & Kamae, 1994; Tumarkin et al., 1994; Archuleta et al., 2003). Empirical Green's functions require the knowledge of stress drop, to scale the observed lower magnitude records at particular receivers (Irikura & Kamae, 1994). The desired range of magnitudes for which to use empirical

Green's functions for $4<M_W<5.5$, due to the fact that earthquakes in this range already exhibit clear radiation patterns.

Prior work has addressed the matter of stress drop variability by estimating this parameter for large earthquake datasets in southern California (Shearer et al., 2006) with $1.6<M_L<3.1$ and worldwide (Allman & Shearer, 2009) with $5.2<M_W<8$. Both Shearer et al. (2006) and Allman & Shearer (2009) used short-period P-waves to fit an exponentially decaying function to the spectra for each earthquake in their catalog using Brune's ω^2 model (1970). Studies show large variability for different magnitudes. Observed stress drop variability may be explainable because of unreliable stress drop estimates due to the large amount of complexities observed in earthquake source rupture phenomena (Lavallée et al., 2006). Interesting findings of Shearer et al. (2006) and Allmann & Shearer (2009) are that the mean and the median of observed stress drops are roughly constant for all magnitudes, roughly ~3MPa, but the stress drop variability is quite large, with a range over 1000 MPa, and magnitude non-dependent. The median stress drop between 8 and 18 km depth is approximately 2.2 MPa and depth dependent. In their map of smoothed stress drops the stress drop decreases going from west (near the Elsinore Fault) —with values near 1.6 to 2.5 MPa— to east near the southern extension of the San Jacinto Fault and the Imperial Fault —with values near 0.6 MPa. The relationship for stress drop and seismic moment is:

$$\Delta\sigma = \frac{7}{16}\frac{M_0}{r^3} \tag{1}$$

where $\Delta\sigma$ is the average stress drop, M_0 is the seismic moment and r is the radius of a circular fault. The radius, r, scales in terms of the corner frequency of the S-wave spectrum, f_c as:

$$r = k\frac{\beta}{f_c} \tag{2}$$

where β is the S wave velocity and k is a constant equal to 0.21 (Madariaga, 1976). Brune (1970, 1971) on the other hand, derived a different value for k, which is ~0.37. Madariaga's relationship is approximately ~5.5 larger than the estimates of stress drop developed by Brune (1970, 1971). When we compare results obtained in this study with the results of Shearer et al. (2006), we will factor in this difference.

In spite of the importance of the range of magnitudes of $4<M_W<5.5$, there is a lack of stress drop observations for this set of earthquakes. Some of the studies that have aimed to fill the void of stress drop observations in the magnitude range of $4<M_W<5.5$ earthquakes are the efforts of: (1) Humphrey & Anderson (1994), which focuses on the Guerrero subduction zone and (2) The M_W 6.5 1992 Big Bear mainshock and aftershock sequence study of Jones and Helmberger (1996), which analyzed stress drops of 18 earthquake events in the eastern Transverse ranges of California.

DATA

There was a rich aftershock sequence following the M_W 7.2 2010 El Mayor earthquake, including over 60 $4<M_W<5.5$ magnitude events. These aftershocks were mainly concentrated at the northern tip of the Paso Superior fault, near the Borrego Valley Downhole Array (BVDA). BVDA is composed of 4 downhole seismic sensors (see Figure 2) at depths of 9, 19, 139 and 238 m, as well as 15 surface instruments across Borrego Valley (Steidl, 2006).

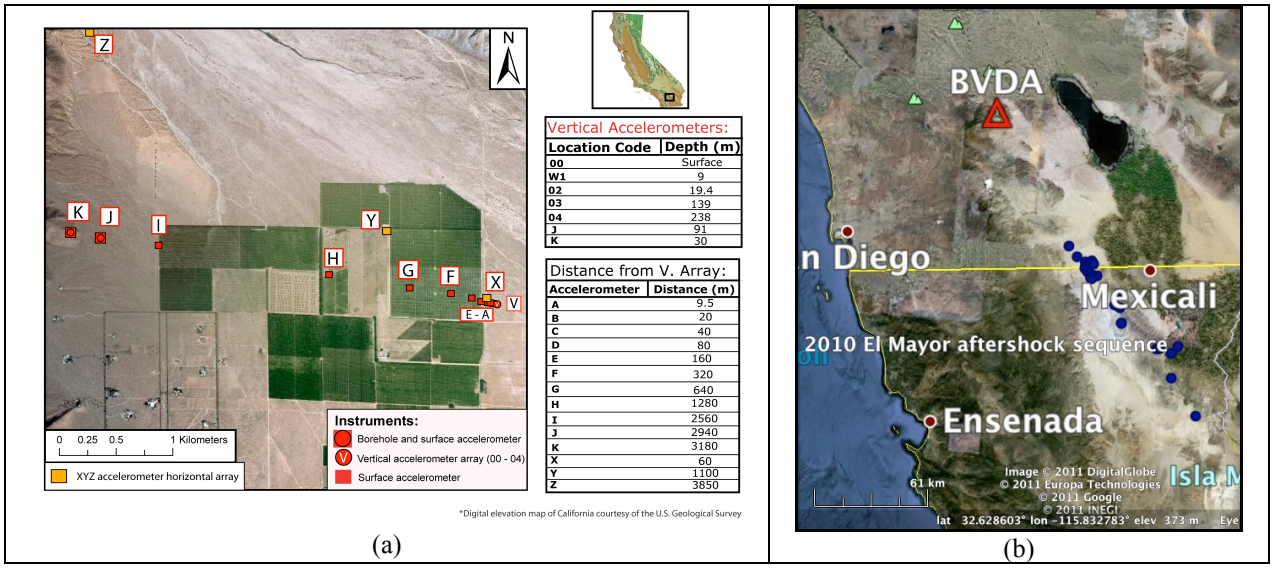

Fig. 1. (a) Location of the BVDA station within California and its geometry (Taken from Steidl, 2006) and (b) Location of the 2010 El Mayor aftershock sequence (blue dots) and BVDA station (red triangle) (map taken from Google Earth).

The locations for the aftershock sequence of the 2010 El Mayor earthquake are depicted in Figure 1. It is possible to observe that the backazimuth of the earthquakes with respect to BVDA is roughly constant. The travel path of seismic waves for the events we analyzed are expected to be similar. We used the EW component of the sensor located at 139 m downhole to compute S-wave spectra for all the events that we have in our catalog.

SOURCE SPECTRAL PARAMETERS

In this study we systematically evaluate stress drops for the selected earthquakes with $4.0<M_W<5.5$ recorded at BVDA. For this we isolated S-wave spectra for each event in our earthquake catalog, from the observed strong ground motion at 139 m downhole. From the S-wave spectra we obtain the corner frequency, which can be related to stress drop, Eqns. 1 and 2. Error analysis shows that a factor of two of uncertainty in both seismic moment and corner frequency, leads to a standard deviation of 6.3 for $\Delta\sigma$ (Pavic et al., 2000). Uncertainty of the corner frequency constitutes 95% of the standard deviation. Corner frequency is affected by the seismic quality factor, especially in the near surface (e.g. Anderson & Hough, 1984), and also by directivity effects (Tumarkin & Archuleta, 1994). Thus using the recorded ground motion at 139 m downhole can avoid near-surface attenuation effects. Higher corner frequencies generally result from directivity effects; this is likely with the 2010 El Mayor mainshock (see Figure 4). Strong directivity effects have been noted at the BVDA station (Graves & Aagaard, 2010) based on numerical simulations of the 2010 El Mayor mainshock. Their simulation was done using a finite element model of the region, incorporating two 3D velocity structure models (CVM-4m and CVM-H62). These velocity models were developed within the framework of the Southern California Earthquake Center (SCEC), for periods of $T > 2$ (s) due to the limitation of computing resources for these numerical methods.

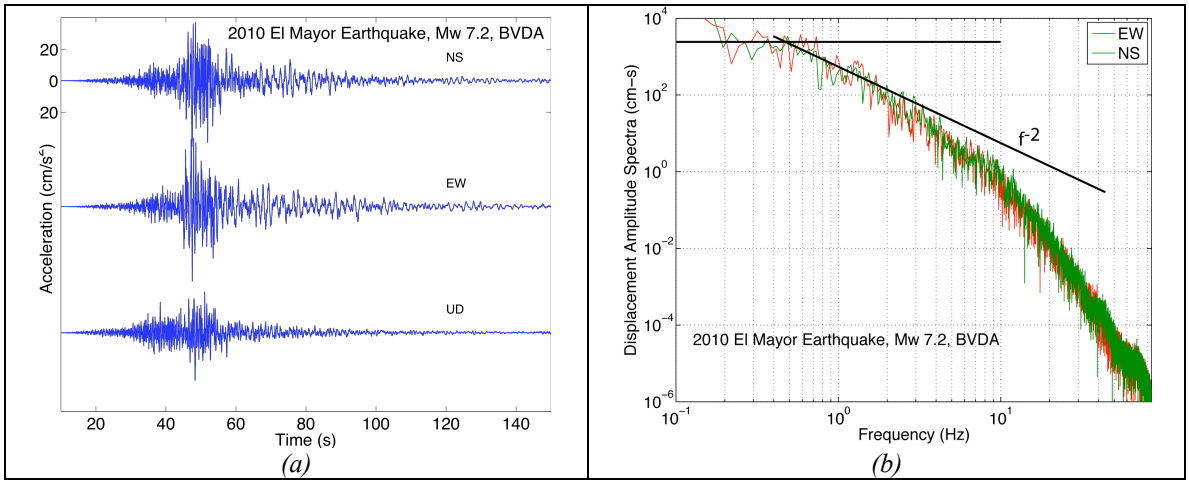

Fig. 2. Accelerograms and horizontal S-wave spectra from the 2010 El Mayor mainshock as recorded at BVDA at the surface. The intersection of the 2 black lines in (b) represents the corner frequency, which is unusually high for an earthquake of this magnitude.

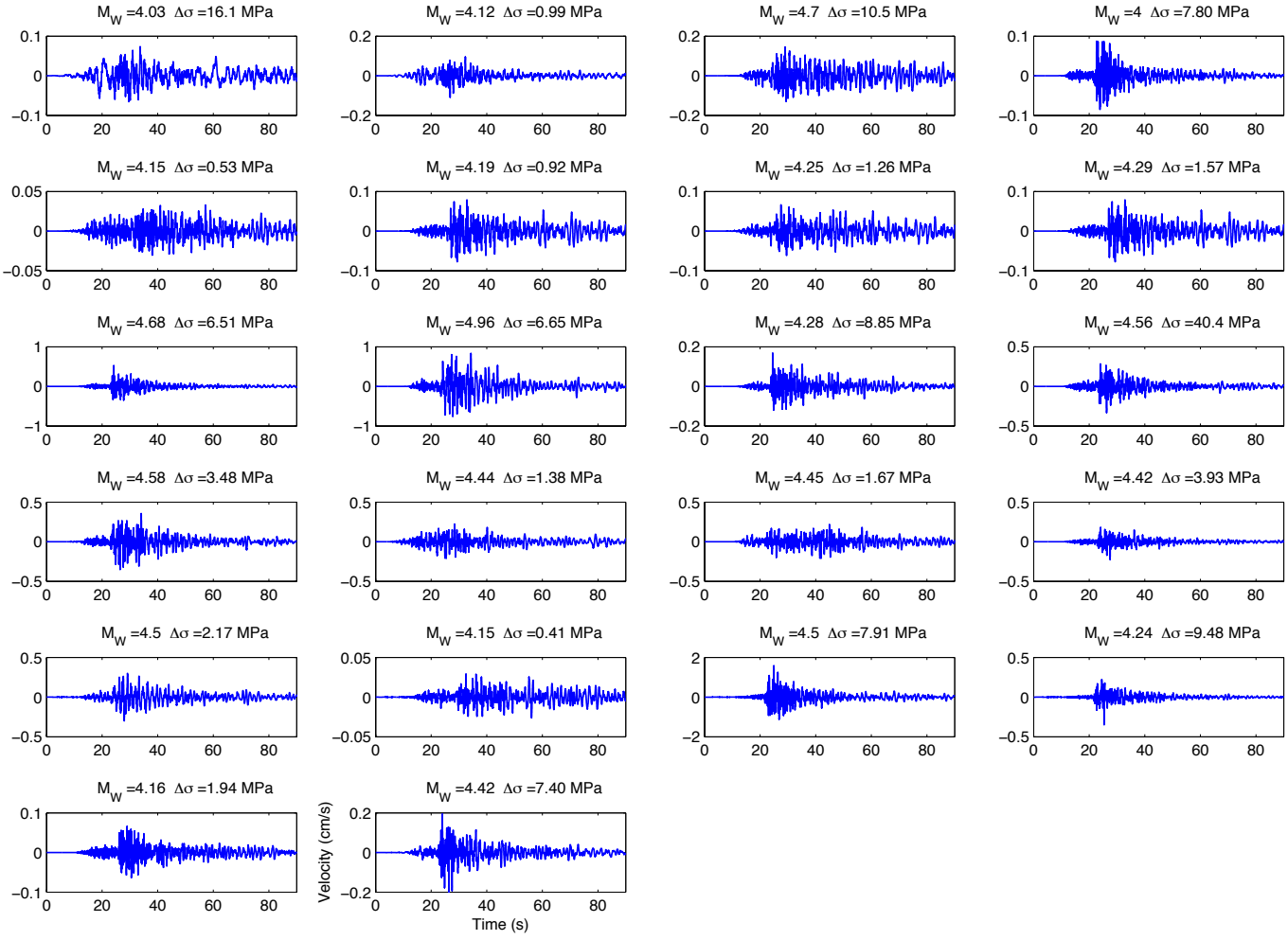

Fig. 3. Velocity time-histories for all 22 analyzed aftershocks.

Figure 3 shows the velocity seismograms at 139 m downhole, with clear S-wave arrivals, which vary approximately from ~25-30 s. From these seismograms, we isolated the S-wave phase using a 5 s Tukey windowing technique, and then corrected for Q effects. For

S-waves, Q is assumed to be ~450, a value that was taken from Hausson and Shearer (2006). Once this was accomplished, we proceeded to compute using the Fast Fourier Transform for the S-wave spectrum for each aftershock event. The model of Boatwright (1978) was used to fit the observed S-wave spectra, which can be written a:

$$\Omega(f) = \frac{\Omega_0}{\left[1+\left(\frac{f}{f_c}\right)^4\right]^{1/2}} \tag{3}$$

A Trust Region method was used as an algorithm to search for the most optimal model (Byrd et al., 2000).

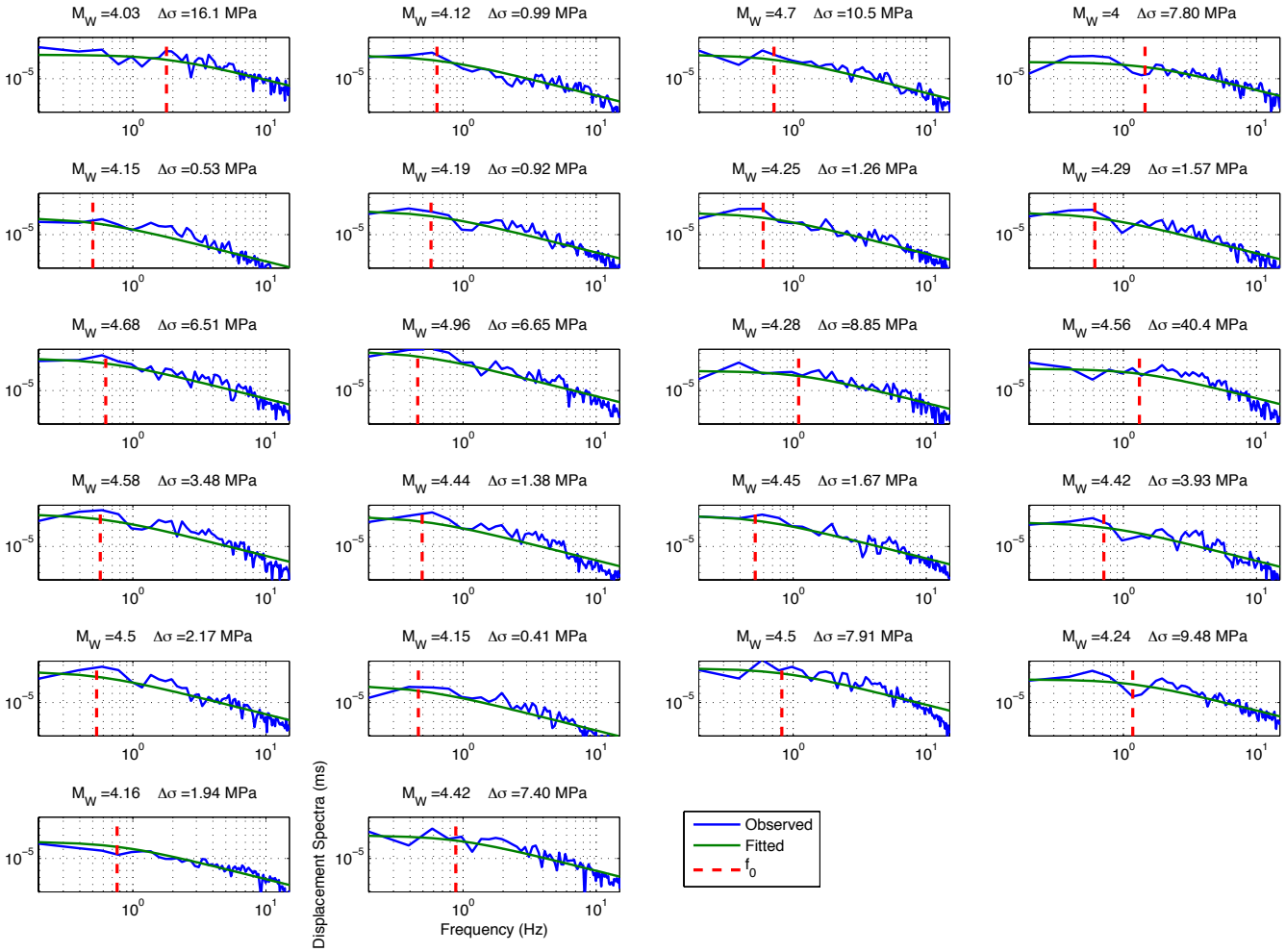

Fig. 4. Displacement amplitude spectra for all 22 analyzed aftershocks (in blue) and the Boatwright (1978) source model fit (in green) are plotted in a log-log format. The corner frequency, f_c is also shown (in dashed red). The calues of frequency range from 0-15 Hz. The values of spectral amplitude are in the range of 10e-08 to 3e-03.

From Figure 4 one can see that at higher frequencies, the spectra falloff has a higher rate than ω^{-2}. To avoid the lowering of the fitted spectrum we only considered spectral information below 15 Hz, which leads to better constrain fits to the true spectra. But in general the fitted spectra seems to be in good agreement with the observed data.

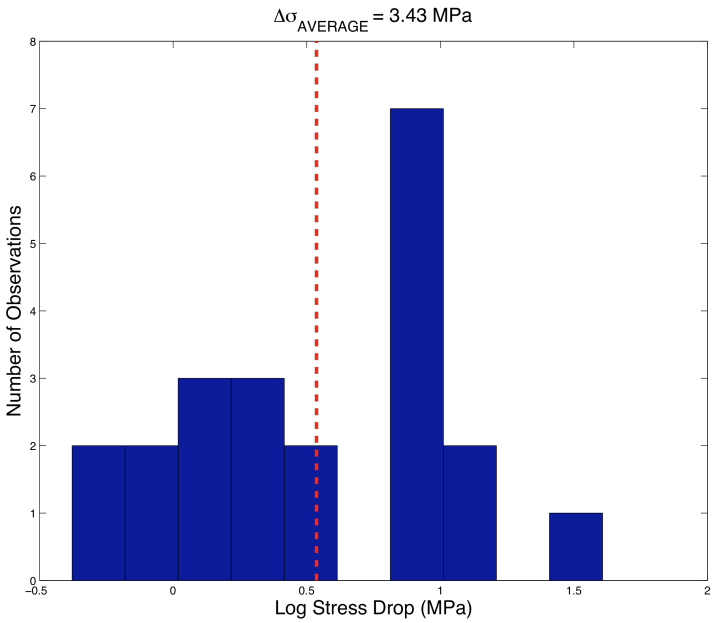

Fig. 5. Histogram that shows the variability of observed stress drops. The average is shown in the red dashed line, with a value of ~3.4 MPa.

Figure 5 shows the large variability of observed stress drops for the 2010 El Mayor aftershock sequence. The range is approximately 40 MPa, with an average value of ~3.4 MPa. This value for average stress drops is approximately ~32 times larger than the values observed by Shearer et al. (2006) for the same region, if one considers that they used Madariaga's (1976) relationship for radius and seismic moment which amplifies 5.5 times with respect to the values of Brune (1970, 1971).

CONCLUSIONS

We have observed values of stress drop, which range from 0.17-40 MPa. This result is quite interesting since the conditions for the aftershocks was quite similar, such as the travel path of the seismic waves and the location of the sources. The highly variable results for stress drops illuminates the complexity of the faulting process on the northern end of the Paso Superior fault. Another repeating observed feature was the relatively low spectral displacement values at higher frequencies. These observations were consistently the same for each aftershock. The average observed stress drop is approximately ~3.4 MPa, a value that is almost 32 times larger than the values reported by Shearer et al. (2006) for the same region.

ACKNOWLEDGMENTS

This work was supported by SCEC. SCEC is funded by NSF Cooperative Agreement EAR-0106924 and USGS Cooperative Agreement 02HQAG0008. Special thanks to Robin Gee for providing us with the BVDA data.

REFERENCES

Abercrombie, R. [1995], Earthquake source scaling relationships from -1 to 5 ML using seismograms recorded at 2.5 km depth, *J. Geophys. Res.*, **100**(240), 15–24,036.

Aki, K. [1967], Scaling law of seismic spectrum, *J. Geophys. Res.*, **72**(4), 1217–1231.

Allmann, B.P. and P.M. Shearer [2009], Global variations of stress drop for moderate to large earthquakes, *J. Geophys. Res.*, **114**(B1), B01310. doi:10.1029/2008JB005821.

Anderson, J., and S. Hough [1984]. A model for the shape of the Fourier amplitude spectrum of acceleration at high frequencies, *Bull. Seismol. Soc. Am.* **74**(5), 1969–1993.

Andrews, D.J. [1980]. A stochastic fault model 1. Static case, *J. Geophys. Res.,* **85**(B7), 3867-3877.

Archuleta, R., E. Cranswick, C. Mueller, and P. Spudich [1982], Source parameters of the 1980 Mammoth Lakes, California, earthquake sequence, *J. Geophys. Res*., **87**(B6), 4595 – 4607.

Archuleta, R. J., P-C Liu, J. H. Steidl, L. F. Bonilla, D. Lavallée, and F. Heuze [2003]. Finite-fault site-specific acceleration time

histories that include nonlinear soil response, *Phys. Earth Planetary Int.*, **137**(1-4), 153-181, doi: 10.1016/S0031-9201(03)00013-X.
Boatwright, J. [1978]. Detailed spectral analysis of two small New York State earthquakes, *Bull. Seismol. Soc. Am.*, **68**, 1117-1131.
Boatwright, J. [2007]. The persistence of directivity in small earthquakes, *Bull. Seismol. Soc. Am*. **97**(6), 1850-1861. doi: 10.11785/0120050228.
Boatwright, J. and D. M. Boore [1982]. Analysis of the ground accelerations radiated by the 1980 Livermore Valley earthquakes for directivity and dynamic source characteristics, *Bull. Seismol. Soc. Am*. **72**(6A), 1843-1866.
Brune, J. N. [1970]. Tectonic stress and the spectra of seismic shear waves from earthquakes, *J. Geophys. Res*., **75**(26), 4997-5009. (correction, ibid, 1971, **76**, 5002.)
Byrd, R.H., J. C. Gilbert, and J. Nocedal [2000], A trust region method based on interior point techniques for nonlinear programming, *Mathematical Programming*, 89(1), 149–185.
Frankel, A. [2009]. A constant stress-drop model for producing broadband synthetic seismograms: Comparison with the Next Generation Attenuation relations, *Bull. Seism. Soc. Am.,* **99**(2A), 664-680, doi: 10.1785/0120080079.
Frankel, A. [1995]. Simulating strong motions of large earthquakes using recordings of small earthquakes: The Loma Prieta mainshock as a test case, *Bull. Seismol. Soc. Am*. **85**(4), 1144–1160.
Graves, R. W. and A. Pitarka [2010]. Broadband ground-motion simulation using a hybrid approach, *Bull. Seismol. Soc. Am*., **100**(5A), 2095-2123.
Graves, R. W. and B. T. Aagaard [2010]. Testing long-period ground motion simulations of scenario earthquakes using the Mw 7.2 El Mayor Cucapah mainshock: Evaluation of finite-fault rupture characterization and 3D seismic velocity models, submitted BSSA, movie at
http://pasadena.wr.usgs.gov/office/rgraves/ElMayorCucapah/ESupp/Movies/rwg_sierra-el-mayor_s1764-v1.3_cvmS4_0.5Hz.mov.
Hanks, T. [1979], b values and ω-γ seismic source models: Implications for tectonic stress variations along active crustal fault zones and the estimation of high-frequency strong ground motion, *J. Geophys. Res*., **84**(B5), 2235–2242.
Hartzell, S. [1978]. Earthquake aftershocks as Green's functions, *Geophys. Res. Lett.*, **5**(1), 1-4.
Hauksson, E., and P. M. Shearer [2006], Attenuation models (Qp and Qs) in three dimensions of the southern California crust: Inferred fluid saturation at seismogenic depths, *J. Geophys. Res.*, 111, B05302, doi:10.1029/2005JB003947.
Humphrey, J.R., Jr. and J. G. Anderson [1994]. Seismic source parameters from the Guerrero subduction zone, *Bull. Seismol. Soc. Am*. **84**(6) 1754-1769.
Hutchings, L. [1994]. Kinematic earthquake models and synthesized ground motion using empirical Green's functions, *Bull. Seismol. Soc. Am*. **84**(4), 1028-1050.
Irikura, K. [1983]. Semi-empirical estimation of strong ground motions during large earthquakes, *Bull. Disas. Prev. Res. Inst., Kyoto Univ*., **33**(2-298), 63-104.
Irikura, K., and K. Kamae [1994]. Estimation of strong ground motion in broad-frequency band based on a seismic source scaling model and an empirical Green's function technique, *Annali di Geofisica*, **37**(6), 1721-1743.
Jones, L. E. and D. V. Helmberger [1996]. Seismicity and stress-drop in the eastern Transverse ranges, Southern California, *Geophys. Res. L.*, **23**(3), 233-236.
Kamae, K., T. Ikeda and S. Miwa [2005]. Source model composed of asperities for the 2004 Mid Niigata Prefecture, Japan, earthquake (MJMA=6.8) by the forward modeling using the empirical Green's function method, *Earth, Planets and Space*, **57**(6), 533-538.
Kanamori, H., and D. Anderson [1975], Theoretical basis of some empirical relations in seismology, *Bull. Seismol. Soc. Am*., **65**(5), 1073–1095.
Lavallée, D., P. Liu, and R. J. Archuleta [2006], Stochastic model of heterogeneity in earthquake slip spatial distributions, *Geophys. J. Int*., **165**(2), 622-640.
Liu H-L and D. V. Helmberger [1985]. The 23:19 aftershock of the 15 October 1979 Imperial Valley earthquake: More evidence for an asperity, *Bull. Seismol. Soc. Am*., **75**(3), 689-708.
Liu, P.C., R.J. Archuleta, & S. Hartzell, [2006]. Prediction of broadband ground-motion time histories: Hybrid low/high-frequency method with correlated random source parameters, *Bull. Seism. Soc. Am,* **96**(6), 2118-2130.
Morozov, I.V. [2010]. On the causes of frequency-dependent apparent seismological *Q*, *Pure and Applied Geophysics*, **167**(10) 1131-1146. doi: 10.1007/s00024-010-0100-6.
McGuire, J. J. [2004]. Estimating the finite source properties of small earthquake ruptures, *Bull. Seismol. Soc. Am.* **94**(2), 377–393.
Olsen, K. B., R. Nigbor and T. Konno [2000]. 3D viscoelastic wave propagation in the upper Borrego Valley, California, constrained by borehole and surface data, *Bull. Seismol. Soc. Am*., **90**(1), 134-150, doi: 10.1785/0119990052.
Pitarka, A., P. Somerville, Y. Fukushima, T. Uetake, and K. Irikura [2000]. Simulation of near-fault strong ground motion using hybrid Green's functions, *Bull. Seismol. Soc. Am*., **90**(3), 566-587.
Pavic, R., M. G. Koller, P-Y. Bard & C. Lacave-Lachet [2000]. Ground motion prediction with the empirical Green's function technique: an assessment of uncertainties and confidence level, *J. Seismology*, **4**(1), 59-77.
Schmedes, J., R. J. Archuleta, and D. Lavallée [2010]. Correlation of earthquake source parameters inferred from dynamic rupture simulations, *J. Geophys. Res.*, **115**(B3), B03304. doi:10.1029/2009JB006689.
Shearer, P., G. Prieto, and E. Hauksson [2006], Comprehensive analysis of earthquake source spectra in southern California, *J.*

Geophys. Res., **111**(B6), B06303, doi:10.1029/2005JB003979.
Steidl, J. [2006]. Geotechnical Array data analysis at Borrego Valley and NEES/ANSS integration, USGS Final Report, 06HQGR0135.
Tumarkin, A. G. and R. J. Archuleta [1994]. Empirical ground motion prediction, *Annali di Geofisica*, **37**(6), 1691-1720.